polysaccharides

MDPI

Article

Surface Modification of Cellulose Nanocrystal Films via RAFT Polymerization for Adsorption of PFAS

Chaimaa Gomri, Belkacem Tarek Benkhaled, Arnaud Chaix, Eddy Petit, Marc Cretin and Mona Semsarilar *

Institut Européen des Membranes-IEM (UMR 5635), Univ. Montpellier, CNRS, ENSCM, 34095 Montpellier, France; chaimaa.gomri@umontpellier.fr (C.G.); belkacem-tarek.benkhaled@umontpellier.fr (B.T.B.); arnaud.chaix@umontpellier.fr (A.C.); eddy.petit@umontpellier.fr (E.P.); marc.cretin@umontpellier.fr (M.C.)
* Correspondence: mona.semsarilar@umontpellier.fr

Abstract: Cellulose nanocrystals (CNCs) are bio-based materials able to be functionalized following different approaches, which expands their range of applications. One such approach is surface-initiated polymerization, which involves the attachment of an initiator to the CNC's surface to initiate the growth of the polymer. This work reports the modification of CNCs using the described approach. First, a CNC-based film was prepared, on which an initiator (RAFT agent) was grafted, and then (trimethylaminoethyl methacrylate, a positively charged monomer, was polymerized using reversible addition–fragmentation chain-transfer (RAFT) polymerization. The CNC film was successfully modified and fully characterized. Different degrees of polymerization were targeted to emphasize the effect of the positively charged polymer and their chain length on the adsorption efficiency. The results showed that by increasing the chain length of the grafted polymer, up to 80% of both pollutants could be removed, with a faster adsorption of PFOS as compared to PFOA.

Keywords: perfluorooctanoic acid (PFOA); perfluorooctanesulfonic acid (PFOS); cellulose nanocrystal (CNC); poly (trimethyl aminoethyl methacrylate) (PTMAEMA); reversible addition–fragmentation chain transfer (RAFT)

Citation: Gomri, C.; Benkhaled, B.T.; Chaix, A.; Petit, E.; Cretin, M.; Semsarilar, M. Surface Modification of Cellulose Nanocrystal Films via RAFT Polymerization for Adsorption of PFAS. *Polysaccharides* **2024**, *5*, 85–95. https://doi.org/10.3390/polysaccharides5020006

Academic Editor: Sergiu Coseri

Received: 8 March 2024
Revised: 9 April 2024
Accepted: 11 April 2024
Published: 13 April 2024

1. Introduction

Cellulose nanocrystals (CNCs) are derived from cellulose, the most abundant biopolymer [1]. CNCs have attracted significant attention in recent years due to their unique properties and potential applications in various fields. They have a high specific surface area, which offers the potential for various functionalization and surface modification techniques [2]. Adding functional groups helps increase CNCs' strength and thermal stability and can improve absorption efficacy. CNCs can be modified through the hydroxyl group present on their surface. Various groups, such as amino, sulfonic, or polymers, can be attached to the surface. The choice of inserted species depends on the intended application [3].

The modification of CNCs by graft polymerization is an interesting approach that has been widely applied to attach a sequence of monomers to a cellulose backbone. "Grafting from" and "grafting to" are the two main approaches commonly used. "Grafting to" involves bonding a pre-synthesized polymer onto the CNC surface. Steric hindrance presents a limitation of this approach, especially for longer polymer chains [4]. In "grafting from", the polymerization initiator is first attached to the CNC surface to enable the growth of the polymer [5]. Analysis of the grafted polymer when using the "grafting from" approach is challenging compared to "grafting to". Atom transfer radical polymerization (ATRP) and reversible addition–fragmentation chain transfer (RAFT) are controlled polymerizations used to graft complex structures to CNC surfaces [6]. For both techniques, an initiator is first grafted, mainly by esterification [7]. 2-Bromoisobutyryl bromide [6] and α-Bromoisobutyric acid [8] are the ATRP initiators that are mainly grafted on CNCs, while

for RAFT, 4-cyano-4-(phenylcarbonothioylthio) pentanoic acid has been extensively used by researchers to graft polymers such as poly (methyl methacrylate) (PMMA) [9], poly (dimethylaminoethyl methacrylate) (PDMAEMA) [10], and so on. For instance, Eskandari et al. grafted N-isopropylacrylamide block (2-dimethylaminoethyl) methacrylate, a temperature-responsive polymer for the absorbance of carbon dioxide (CO_2), using RAFT polymerization [11]. The group was able to test different lengths of the block's polymers. In general, grafting enhances the versatility of CNCs and enlarges their application in a long list of fields, such as electronics [12], water treatment [13], packaging [14], biomedicine [15], among others. In this context, we studied the chemical modification of CNCs with a functional amine polymer synthesized via RAFT polymerization. First, a film was made from CNCs; then, the surface of the film was modified via grafting a RAFT agent by silylation. This modification was governed by the interaction between the hydroxyl group of the CNCs and the methoxysilane group present on the RAFT agent. Then, trimethylaminoethyl methacrylate "TMAEMA" was polymerized with different lengths from the surface of the CNC film. The modified film was fully characterized to confirm the grafting. The developed film was tested to adsorb perfluorooctanoic acid (PFOA) and perfluorooctane sulfonic acid (PFOS). These pollutants belong to the PFAS (per- and poly-fluoroalkyl substances) family. They are hazardous and prominent pollutants that are extensively used, which leads to widespread contamination of the environment, particularly surface and groundwater, which is a direct pathway to human exposure [16,17].

2. Materials and Methods

2.1. Materials

Cellulose nanocrystal (CNC), kindly provided by CelluForce Inc. Canada, was used with polyethylene glycol (PEG) (Sigma-Aldrich, France, M_W~20,000) to prepare films. Cyanomethyl [3-(trimethoxysilyl) propyl] trithiocarbonate (Sigma-Aldrich, 95%) was used as a chain transfer agent. 2-(Dimethylamino) ethyl methacrylate (DMAEMA) (Sigma-Aldrich, 98%) was used as a monomer. Azobisisobutyronitrile (AIBN) was used as the radical initiator. Perfluorooctanoic acid (PFOA) (Sigma-Aldrich, 95%) and perfluorooctanesulfonic acid (PFOS) (Sigma-Aldrich, ~40% in H_2O) were used as the model compounds of the PFAS family.

2.2. Preparation of CNC Film

For the preparation of the CNC film, 0.4 g (80 wt %) of CNC was dispersed with 0.1 g (20 wt %) of PEG in 15 mL of water, sonicated for 10 min, stirred for 24 h, then poured into a mold and dried at room temperature.

2.3. Modification of CNC Film with RAFT Agent (CNC-g-CTA)

To grow the polymer from the CNC film, the RAFT agent was first grafted onto the film surface. For this, 0.5 g of CNC film was placed in a round-bottom flask; then, 0.2 mL (0.783 mmol) of cyanomethyl [3-(trimethoxysilyl) propyl] trithiocarbonate, 40 mL of toluene, and 0.2 mL of dimethylformamide (DMF) were added. The mixture was heated under reflux in an oil bath at 120 °C for 24 h. Afterward, the film was washed with ethanol and dried under vacuum at 40 °C. The degree of substitution of CNC was calculated following Equation (1).

$$DS = \frac{n\,(grafted\ CTA)}{n(CNC)} \quad (1)$$

2.4. Quaternization of DMAEMA

DMAEMA was first modified using iodomethane to quaternize the amine in order to have a permanent positive charge on the monomer (TMAEMA). An amount of 10 g (63 mmol) of DMAEMA was placed in a beaker containing water and placed into an ice bath.

Then, CH_3I (13.54 g, 95 mmol) was added dropwise in excess. After stirring for 2 h, the final product was freeze-dried. The modification was confirmed by ^1H NMR.

2.5. Polymerization of TMAEMA from CNC-g-CTA

The CTA-modified CNC film was placed in a round-bottom flask (20 mg) along with AIBN (15 mg), TMAEMA (Table 1), and dimethylformamide (30 mL). The mixture was sealed, purged by bubbling nitrogen, and heated at 70 °C for 24 h. Different concentrations of the monomer were used to target different degrees of polymerization. The list of different samples prepared can be found in Table 1.

Table 1. Targeted degree of polymerization (DP) with the corresponding sample reference.

Samples	m (g)	n (mmol)	Target Dp
CNC-*g*-PTMAEMA 1	0.2	0.66	40
CNC-*g*-PTMAEMA 2	0.1	0.33	20
CNC-*g*-PTMAEMA 3	0.05	0.16	10

2.6. Adsorption Experiments

To evaluate the adsorption efficiency of the modified CNC film, 20 mg of each sample (CNC-*g*-PTMAEMA 1, CNC-*g*-PTMAEMA 2, and CNC-*g*-PTMAEMA 3) was placed in an aqueous solution (50 mL) of 10 ppm of PFOA (pH = 6.5). The solutions were stirred for 24 h. The adsorption kinetics was evaluated by fitting the results into the linear form of the pseudo-first-order model and pseudo-second-order model using Equations (2) and (3):

$$\ln(q_e - q_t) = \ln(q_e) - K_1 t \quad (2)$$

$$\frac{t}{q_t} = \frac{1}{K_2\, q_e^2} + \frac{t}{q_e} \quad (3)$$

q_e is the equilibrium adsorption capacity, K_1 (min^{-1}) is the constant of the pseudo-first-order model, and K_2 ($g\ mg^{-1}\ min^{-1}$) is the constant of the pseudo-second-order model.

To compare the adsorption of PFOA and PFOS, 20 mg of CNC-*g*-PTMAEMA 1 was placed in an aqueous solution (50 mL) of 10 ppm of PFOS (pH = 6.5), and the solution was stirred for 24 h.

Adsorption isotherms of CNC-*g*-PTMAEMA 1 were evaluated using the Langmuir and Freundlich linear models, Equations (4) and (5), respectively. The concentrations used ranged from 20 ppm to 200 ppm of PFOA (pH = 6.5), and they were stirred for 24 h.

$$\frac{C_e}{q_e} = \frac{C_e}{q_m} + \frac{1}{q_m K_L} \quad (4)$$

$$\ln(q_e) = lnK_f + \frac{1}{n} lnC_e \quad (5)$$

C_e and q_e are the concentration and the quantity adsorbed, respectively, at the equilibrium, q_m is the maximum quantity adsorbed, K_L is the Langmuir constant, K_f is the Freundlich constant, and $\frac{1}{n}$ is the heterogeneity factor.

2.7. Characterization

Thermogravimetric analysis (TGA) was accomplished by TA instruments SDT Q600. Samples were heated from 25 °C to 1000 °C under air with a 10 °C/min ramp.

Proton nuclear magnetic resonance (NMR) analysis was applied on a Bruker Advance spectrometer 400 MHZ at room temperature using $CDCl_3$ as solvent.

Scanning electron microscopy (SEM, Hitachi S-4800) was used at an accelerating voltage of 5 kV to obtain top-view images.

Fourier-transform infrared (FTIR) spectra were obtained using a Thermo Nicolet Nexus FTIR spectrometer with a diamond ATR attachment. Samples were scanned 32 times in the range of 4000 cm^{-1} to 650 cm^{-1}, with a resolution of 4 cm^{-1}.

PFOA and PFOS adsorption was evaluated by high-performance liquid chromatography coupled to mass spectroscopy (HPLC-MS). Electrospray ionization was operated in negative mode for the detection. Quantitative analysis was carried out by using the multiple reaction monitoring mode. The instrument was equipped with a Waters-Xselect HSST3 100 × 2.1 mm column with a 2.5 μm particle size. The injected volume was 1 μL. The mobile phase comprised buffer A (water + 0.1% formic acid) and buffer B (acetonitrile + 0.05% formic acid) with a constant flow rate of 0.25 mL min^{-1}.

3. Results and Discussion

CNC characterization is presented in the previous work [18]; TEM analysis of the CNC showed a diameter of 11 nm and a length of 153 nm. A CNC-based film was prepared by casting a solution of a blend of CNC and PEG. The CNC was mixed with PEG in water and subjected to stirring for 24 h, then cast into a mold and dried at room temperature. PEG was added to give more flexibility to the film. The prepared film showed great stability in organic solvents such as toluene and tetrahydrofuran (THF); it did not swell or disintegrate, even after long exposure, unlike when it was placed in water. The film was then put in a round-bottom flask, where cyanomethyl [3-(trimethoxysilyl) propyl] trithiocarbonate and toluene were added, and a drop of DMF was added as a heterogenous reference for ^{1}H NMR. The mixture was heated under reflux for 24 h at 120 °C. The reaction is illustrated in Figure 1a, and the reaction yield was calculated by ^{1}H NMR. Figure 1b presents the ^{1}H NMR spectrum of [3-(trimethoxysilyl) propyl] trithiocarbonate; the signals at 4.09 ppm, 3.50 ppm, 3.38 ppm, 1.78 ppm, and 0.70 ppm correspond, respectively, to CN-C**H**$_2$-S-, -S-C**H**$_2$-CH$_2$-, -CH$_2$-C**H**$_2$-CH$_2$-, -CH$_2$-C**H**$_2$-Si-, and -Si-O-C**H**$_3$. Figure 1c,d present the proton signals of -Si-O-C**H**$_3$ before and after the reaction, respectively. By comparing the integral of these signals using the DMF signal as a reference, a yield of 62% was calculated, implying a degree of substitution of 0.2. So, for 5 units of glucopyranose of CNC, one molecule of RAFT agent will be grafted. After the insertion of the RAFT agent on the CNC film surface, the latter changed color from transparent to yellow, as seen in Figure S1.

To prepare the permanent positively charged moiety, the commercially available 2-(Dimethylamino) ethyl methacrylate (DMAEMA) was reacted with iodomethane to obtain 2-(Trimethylamino) ethyl methacrylate (TMAEMA), as illustrated in Figure 2a. The reaction was held for 2 h at ambient temperature. The modification was confirmed by ^{1}H NMR; the signal integral for -N-C**H**$_3$- was 6.04 before modification, as shown in Figure 2b. In contrast, after modification, the integral increased to 9.08, thus confirming a reaction yield of 100%, implying a total quaternization of the amino groups of the DMAEMA.

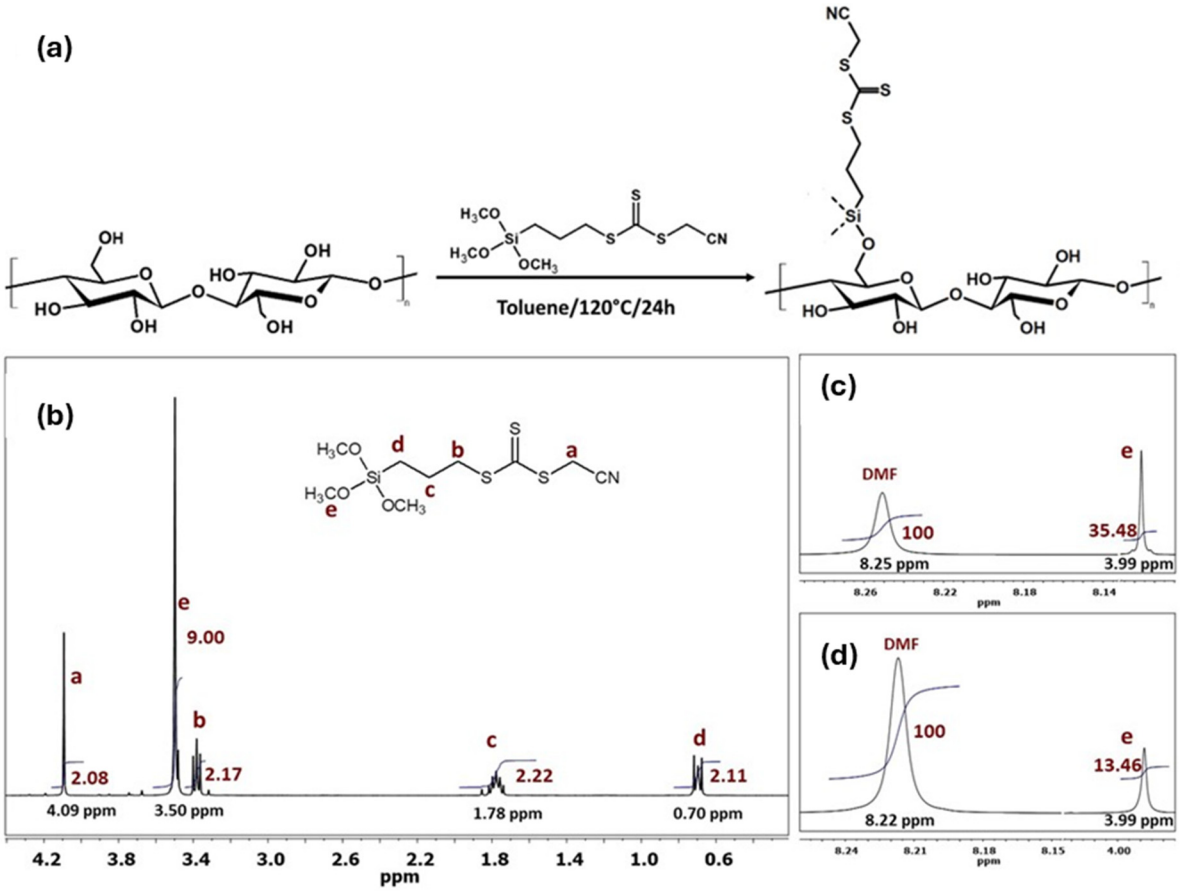

Figure 1. (**a**) Schematic representation of the reaction between CNC and the RAFT agent. (**b**) ^{1}H NMR spectrum of the RAFT agent. (**c**) ^{1}H NMR signal of Si-O-CH_3 before and (**d**) after the reaction.

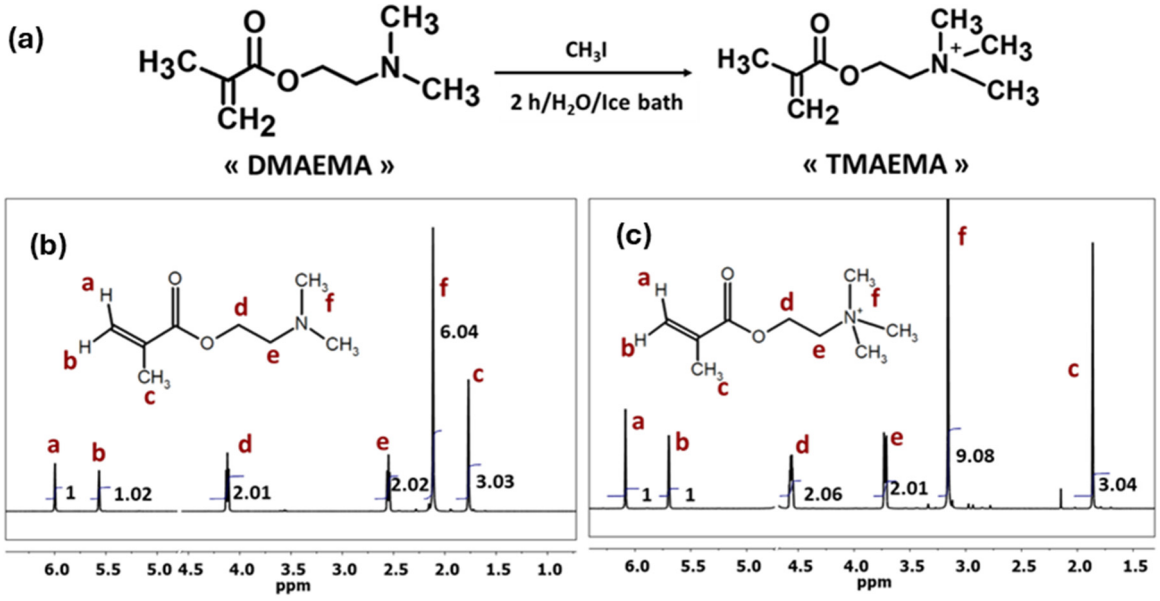

Figure 2. (**a**) Schematic representation of the quaternization reaction of DMAEMA, (**b**) ^{1}H NMR spectrum of DMAEMA before the reaction, and (**c**) after the reaction (TMAEMA).

The TMAEMA monomer was then polymerized from the modified CNC film surface using the RAFT Z-group approach, as illustrated in Figure 3.

Three different degrees of polymerization were targeted: 40, 20, and 10. The obtained DP was calculated by ^{1}H NMR, using DMF as a reference. Figure S2 presents the signals

of the vinyl protons of TMAEMA, before and after the reaction. The obtained DP was calculated using Equation (6):

$$DP_{obt} = Dp_{Targ} \times (1 - \frac{H_{int}after}{H_{int}before}) \quad (6)$$

where H_{int} presents the integral corresponding to vinyl protons before and after the reaction; the DPs obtained were 25, 9, and 4, labeled as CNC-*g*-PTMAEMA 1, CNC-*g*-PTMAEMA 2, and CNC-*g*-PTMAEMA 3, respectively. The reaction yield of CNC-*g*-PTMAEMA 1 was 61%, which is higher than the other samples, where the yields were 45% and 40%, corresponding, respectively, to CNC-*g*-PTMAEMA 2 and CNC-*g*-PTMAEMA 3. Enhancing TMAEMA's quantity led to a higher yield, which can be explained by the fact that the diffusion of the monomer to the CNC film was favored when the reaction medium was concentrated, increasing the probability that the monomer would become attached to the surface of the CNC film. Unfortunately, SEC analysis could not be performed as the PTMAEMA chains grown from the CNC film could not be cleaved and analyzed; cleavage requires strong acidic or basic conditions, which can induce the degradation of the polymer too [10]. However, there are several examples of RAFT-controlled polymerization of TMAEMA in solution using a trithio-based RAFT agent. In a previous work elaborated by Semsarilar et al., where the group polymerized TMAEMA using 4-cyano-4-(2-phenylethanesulfanylthiocarbonyl) sulfanylpentanoic acid, the obtained dispersity index was 1.15, thus confirming well-controlled polymerization [19]. Hence, we believe that the cyanomethyl [3-(trimethoxysilyl) propyl] trithiocarbonate RAFT agent tethered to the CNC film should control the polymerization of TMAEMA.

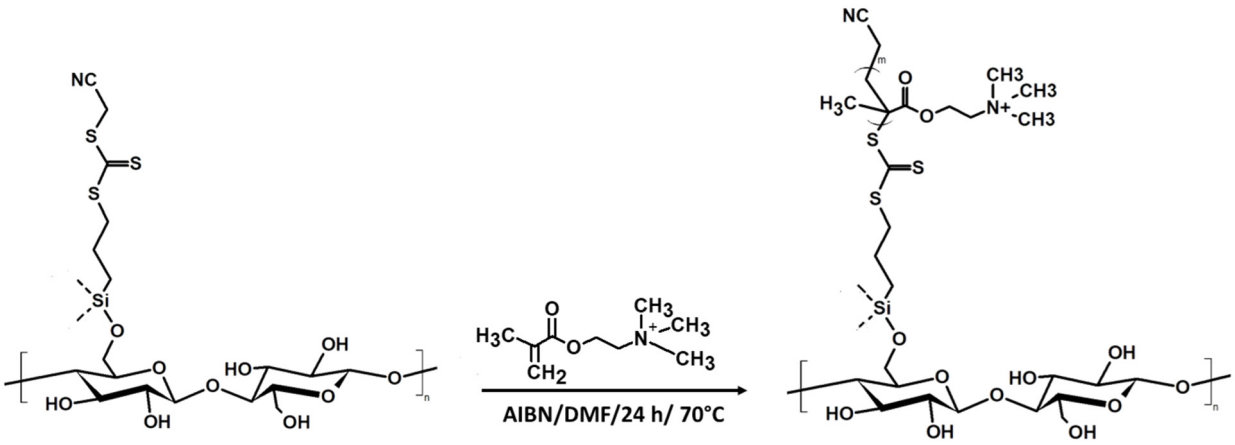

Figure 3. Schematic representation of the TMAEMA grafting from the surface of CNC film.

The grafting was also confirmed with TGA and FTIR analysis. In Figure 4a, the degradation curve of CNC film is different from CNC-g-RAFT and CNC-*g*-PTMAEMA 1. The thermal stability of the film increased after modification. The degradation of the CNC film starts from 200 °C, while for CNC-g-RAFT, 10% is degraded at 100 °C, corresponding to DMF; then, 65% of the film is degraded at 250 °C and the rest is decomposed at 500 °C. Regarding CNC-g-PTMAEMA 1, the degradation curve looks more like that of CNC-g-RAFT, except that the major loss starts from 290 °C instead of 250 °C, and the second degradation slot starts from 540 instead of 500 °C. Zhu et al. confirmed in their work that the thermal stability of CNC increases after modification using an organosilane compound; the group observed that the degradation temperature increased from 285 °C to 325 °C (under nitrogen) after grafting 3-(2-aminoethylamino)-propylmethyldimethoxy silane on CNC [20]. Here, the thermal stability increased due to the insertion of the RAFT agent and the polymer; when grafting these elements onto the CNC, the structure became more complex, which required more energy for degradation.

Figure 4b presents the FTIR spectra of the modified and unmodified CNC films. At 2877 cm^{-1}, a new peak appears for the CNC-*g*-CTA and CNC-*g*-PTMAEMA spectra; this new peak belongs to the C-H bond of CH_2 present in the CTA agent and TMAEMA. Another new peak appears at 1727 cm^{-1} for the CNC-*g*-PTMAEMA, indicating the presence of C=O in the structure of the PTMAEMA (the stretching of C=O).

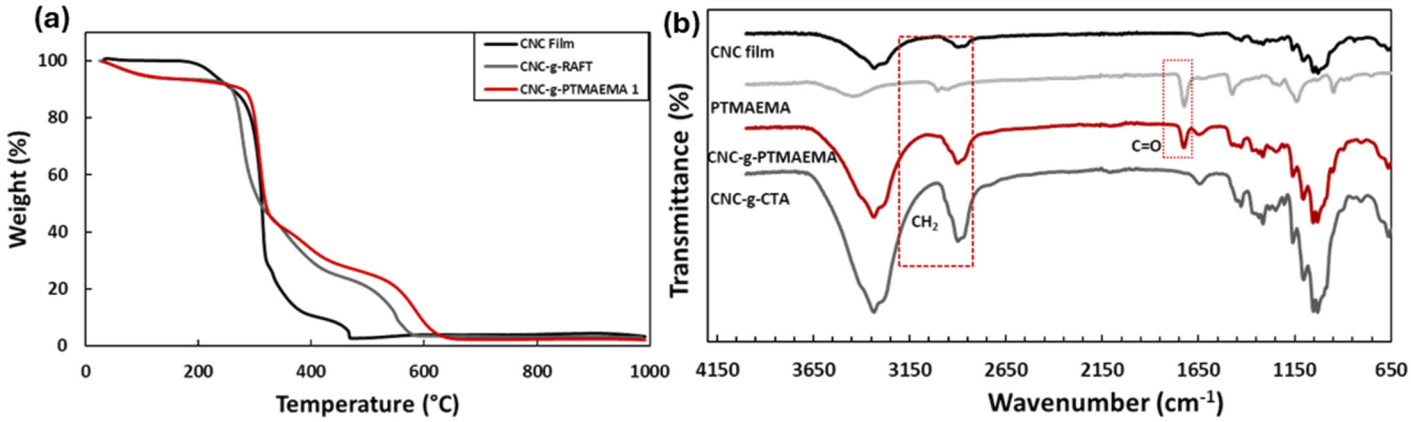

Figure 4. (**a**) TGA analysis. (**b**) FTIR analysis.

Figure 5a shows the smooth surface of the CNC film. However, after grafting the CTA, the surface became coarse (Figure 5b). The roughness increased once the polymer chains were grown from the surface of the film (Figure 5c). In Figure 5d, the grafted moieties show a spherical-liked shape with a diameter of 0.14 µm. Moreover, the developed film shows great resistance in water after modification, contrary to the pristine CNC film that dispersed when it was placed in water (Figure S3). Additionally, the film was exposed to methanol and was sonicated for regeneration tests more than once. Despite all of this, the CNC-g-PTMAEMA film kept its integrity and still could be used for a further absorbance test (Figure S3C). The ability of the modified CNC film to not disperse in water is due to the RAFT agent. The latter belongs to the organosilane family. The insertion of these compounds into a matrix such as CNC is known to enhance the mechanical properties of the material [21]. Moreover, it is hydrophobic, which explains why the film is no longer wettable [22].

A kinetic study of the adsorption of PFOA was carried out on the different samples prepared with different degrees of polymerization. The results were fitted in pseudo-first-order and pseudo-second-order kinetic models (Table 2). All samples followed the pseudo-second-order model, with a correlation coefficient of $R^2 = 0.99$. The best results were obtained with the modified CNC film, which bore the longest grafted PTMAEMA chains (CNC-*g*-PTMAEMA 1).

Table 2. Adsorption kinetic parameters of PFOA.

Samples	q_e Experimental (mg g^{-1})	Pseudo-First-Order			Pseudo-Second-Order		
		q_e (mg g^{-1})	K_1 (h^{-1})	R^2	q_e (mg g^{-1})	K_2 (g mg^{-1} h^{-1})	R^2
CNC-*g*-PTMAEMA 1	17.25	13.50	0.09140	0.96	19.01	0.01065	0.99
CNC-*g*-PTMAEMA 2	7.95	3.87	0.08870	0.65	8.18	0.06766	0.99
CNC-*g*-PTMAEMA 3	4.09	5.68	0.49040	0.87	4.21	0.11918	0.99

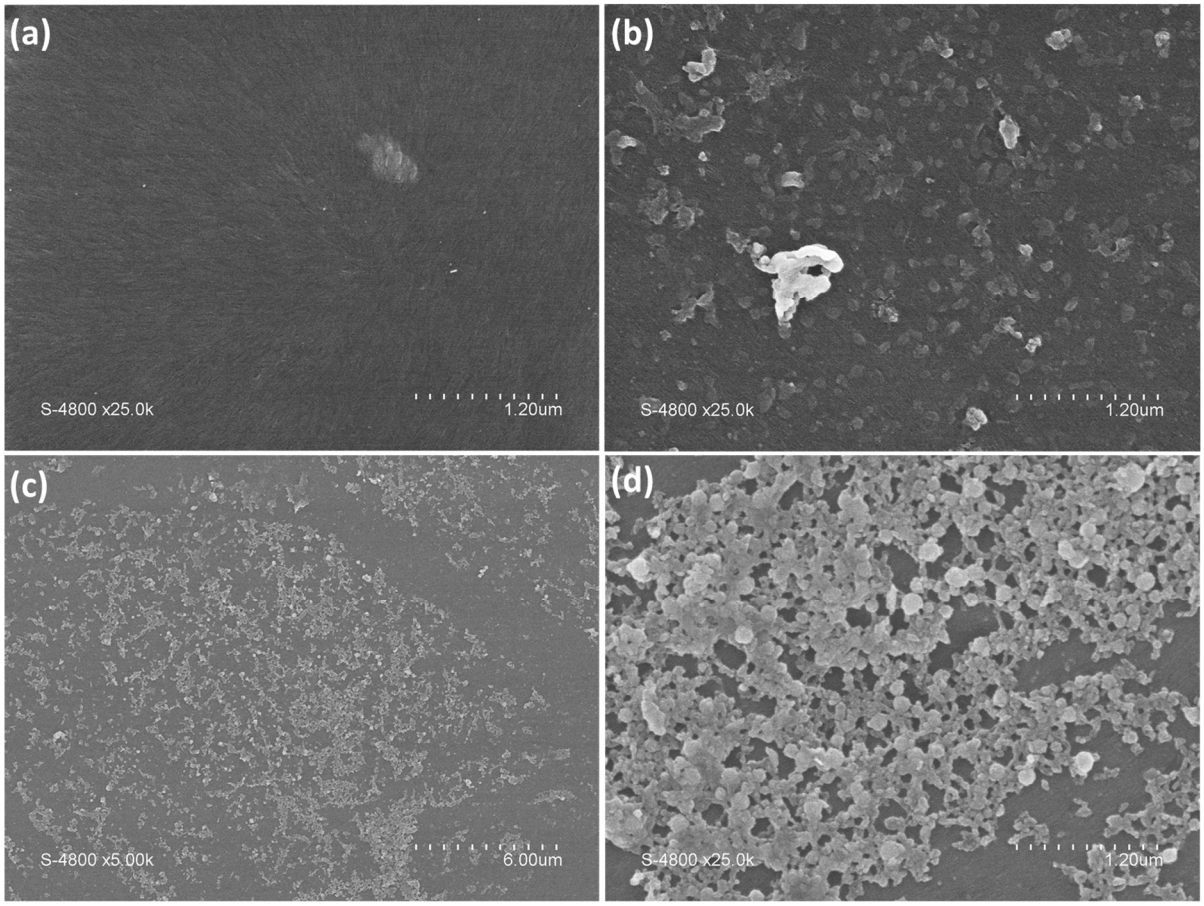

Figure 5. SEM images of (**a**) CNC film, (**b**) CNC–g–CTA, (**c**) CNC–g–PTMAEMA 1 (scale bar = 6 μm), and (**d**) CNC–g–PTMAEMA (scale bar = 1.2 μm).

The removal percentages for each sample, CNC-*g*-PTMAEMA 1, CNC-*g*-PTMAEMA 2, and CNC-*g*-PTMAEMA 3, were 80%, 41.5%, and 24%, respectively (Figure 6a). The adsorption rate of PFOA was higher for CNC-*g*-PTMAEMA 1. A total of 50% of PFOA was removed after 5 h, while for the other samples, more than 60% remained. By increasing the length of the grafted polymer, the quantity of PFOA adsorbed at the equilibrium and the adsorption rate increased, while the equilibrium rate constant of the pseudo-second-order constant kinetics K_2 decreased, as shown in Figure 6b. Based on the equation of the pseudo-second order, the kinetic constant K_2 is inversely related to the sorption rate [23], which is in correlation with the obtained results; when the adsorption rate increases, K_2 values tend to decrease.

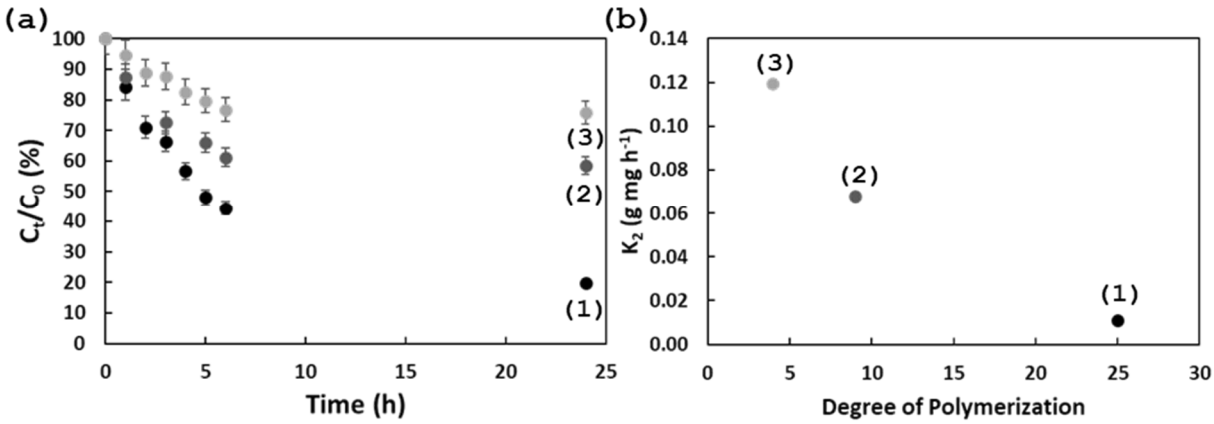

Figure 6. (**a**) Variation in C_t/C_0 (PFOA) as a function of time (h) for the different samples (1) CNC–g–PTMAEMA 1, (2) CNC–g–PTMAEMA 2, and (3) CN–g–PTMAEMA 3. (**b**) Variation in equilibrium rate constant K_2 as a function of polymerization degree.

The kinetic constant of the adsorption of PFOS was also studied to compare the affinity of the two pollutants to be adsorbed on the polymer-grafted CNC film (CNC-*g*-PTMAEMA 1). As seen in Figure 7, both pollutants reached equilibrium after 24 h, with 80% removal of PFOA and PFOS, although during the first hour, 40% of PFOS was removed, while only 20% of PFOA was removed. This is certainly due to the fact that adsorption occurs via the acid/base interaction (oppositely charged electrostatic interactions) between the pollutant and the grafted polymer chains. The sulfonic groups, a strong acid, have more affinity towards the quaternized amine groups as compared to the carboxylic group (a weak acid). In the same adsorption conditions, granulated activated carbon showed slower kinetics (120 h to reach equilibrium [23]) compared to CNC-*g*-PTMAEMA, which was only 24 h. Another advantage of film adsorbents is that they can be easily handled during the adsorption/desorption process compared to other adsorbent forms.

Adsorption isotherms were investigated by fitting the adsorption test results into the Langmuir and Freundlich models (Table 3). For this, different PFOA concentrations ranging from 20 ppm to 200 ppm were used. The results best fitted the Freundlich model with a correlation coefficient of $R^2 = 0.96$, with 1/n being 0.81, and a Freundlich constant of 8.45 $((mg\ g^{-1})\ (L\ mg^{-1}))^{1.23}$. The Freundlich model assumes multilayer adsorption; the first adsorption happens via the electrostatic interaction between the positively charged amine of the modified CNC film and the negatively charged functional group of the pollutants; then, another layer of the pollutant is adsorbed via the hydrophobic interaction between the fluorine atoms.

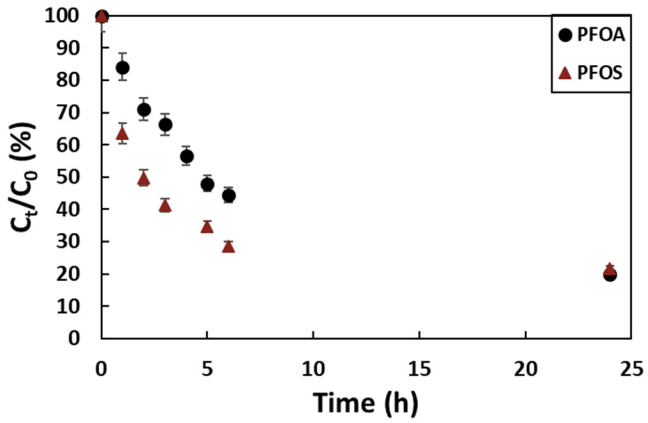

Figure 7. Variation in C_t/C_0 (PFOA and PFOS) as a function of time (h) for CNC-g-PTMAEMA 1.

Table 3. Langmuir and Freundlich parameters of PFOA adsorption on CNC-g-PTMAEMA 1.

Sample	Langmuir Model			Freundlich Model		
CNC-*g*-PTMAEMA 1	K_L (L mg^{-1})	q_m (mg g^{-1})	R^2	Kf $((mg\ g^{-1})\ (L\ mg^{-1})^{1/n}$	1/n	R^2
	0.0375	227	0.91	8.45	0.81	0.96

The ability of a material to be re-generated is an important parameter to consider for practical use. To evaluate the capacity of the developed material to be reused, 40 mg of the CNC-*g*-PTMAEMA 1 film was placed in a beaker containing a solution of PFOA (50 mL, 5 mg L^{-1}) for 24 h. The film was then placed in a beaker with 50 mL of methanol, sonicated for 30 min, and kept under stirring for 48 h. After drying, the material was reused for adsorption. The adsorption/desorption cycles were repeated several times. The obtained results are illustrated in Figure 8. The material showed a very good tolerance towards the cleaning process. In all four cycles, the rate of adsorption was higher than

90%, demonstrating that the film can keep being used and cleaned over time without losing its capacity and performance in adsorbing the pollutants.

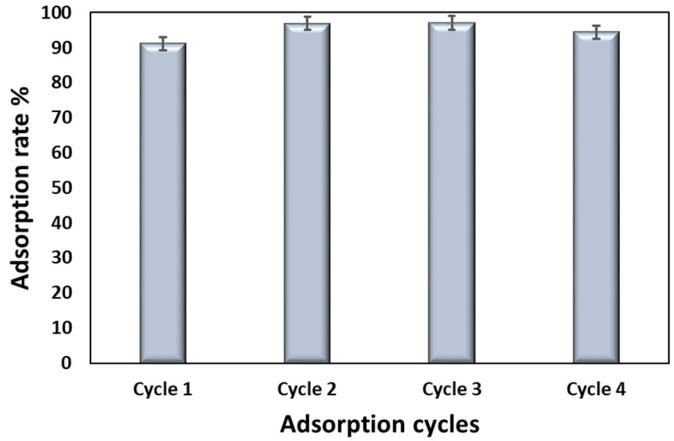

Figure 8. Regeneration cycle of CNC-g-PTMAEMA 1 film versus adsorption rate of PFOA.

4. Conclusions

CNC is a promising material with good mechanical and chemical properties and is able to replace some petroleum-based materials. The presence of a hydroxyl group on its surface makes it suitable for modification, depending on the intended application. Herein, a new adsorbent based on grafting a polymer from a CNC film is developed. Different lengths of grafted polymer chains were evaluated. The film with the highest DP (longer grafted polymer chains) had the best capacity and affinity to adsorb both PFOA and PFOS. As expected, the rate of adsorption of PFOS was higher than that of PFOA. The adsorption kinetics followed the second-order degree, with a kinetics constant (K_2) that decreased with increasing polymer DP. The adsorption isotherm followed the Freundlich model, indicating multilayer adsorption.

Furthermore, this new adsorbent could be regenerated and reused while maintaining its original adsorption capacity. These data suggest that the presented new adsorbents are very efficient and reliable for the removal of PFAS molecules from the environment.

Supplementary Materials: The following supporting information can be downloaded at: https://www.mdpi.com/article/10.3390/polysaccharides5020006/s1, Figure S1: Digital images of CNC film A. Before modification and B. After grafting the polymer (CNC-g-PTMAEMA 1); Figure S2: 1H NMR signals of vinyl protons of CNC-g-PTMAEMA 1 before (a) and after (b), CNC-g-PTMAEMA 2 before (c) and after (d), and CNC-g-PTMAEMA 3 before (e) and after (f) the reaction; Figure S3: A. and B. Digital images of CNC-g-PTMAEMA 1 film in water (left) and dispersed CNC film. C. CNC-g-PTMAEMA 1 film after several generation tests using sonication and methanol.

Author Contributions: Conceptualization, C.G.; Methodology, C.G.; Validation, B.T.B.; Formal analysis, E.P.; Investigation, B.T.B. and A.C.; Resources, M.S.; Data curation, C.G. and B.T.B.; Writing – original draft, C.G.; Writing – review & editing, C.G., B.T.B., M.C. and M.S.; Supervision, M.C. and M.S.; Funding acquisition, M.S. All authors have read and agreed to the published version of the manuscript.

Funding: This research received no external funding.

Institutional Review Board Statement: Not applicable.

Data Availability Statement: Additional material is available in the Supplementary Materials. The raw data supporting the conclusions of this article will be made available by the authors on request.

Conflicts of Interest: The authors declare no conflict of interest.

References

1. Garcia-Valdez, O.; Champagne, P.; Cunningham, M.F. Graft modification of natural polysaccharides via reversible deactivation radical polymerization. *Prog. Polym. Sci.* **2018**, *76*, 151–173. https://doi.org/10.1016/j.progpolymsci.2017.08.001.
2. Lagerwall, J.P.F.; Schütz, C.; Salajkova, M.; Noh, J.; Park, J.H.; Scalia, G.; Bergström, L. Cellulose nanocrystal-based materials: From liquid crystal self-assembly and glass formation to multifunctional thin films. *NPG Asia Mater.* **2014**, *6*, e80. https://doi.org/10.1038/am.2013.69.
3. George, J.; Sabapathi, S.N. Cellulose nanocrystals: Synthesis, functional properties, and applications. *Nanotechnol. Sci. Appl.* **2015**, *8*, 45–54. https://doi.org/10.2147/NSA.S64386.
4. Roy, D.; Semsarilar, M.; Guthrie, J.T.; Perrier, S. Cellulose modification by polymer grafting: A review. *Chem. Soc. Rev.* **2009**, *38*, 2046–2064. https://doi.org/10.1039/b808639g.
5. Semsarilar, M.; Perrier, S. "Green" reversible addition-fragmentation chain-transfer (RAFT) polymerization. *Nat. Chem.* **2010**, *2*, 811–820. https://doi.org/10.1038/nchem.853.
6. Oberlintner, A.; Likozar, B.; Novak, U. Hydrophobic functionalization reactions of structured cellulose nanomaterials: Mechanisms, kinetics and in silico multi-scale models. *Carbohydr. Polym.* **2021**, *259*, 117742. https://doi.org/10.1016/j.carbpol.2021.117742.
7. Gomri, C.; Cretin, M.; Semsarilar, M. Recent progress on chemical modification of cellulose nanocrystal (CNC) and its application in nanocomposite films and membranes-A comprehensive review. *Carbohydr. Polym.* **2022**, *294*, 119790. https://doi.org/10.1016/j.carbpol.2022.119790.
8. Arredondo, J.; Jessop, P.G.; Champagne, P.; Bouchard, J.; Cunningham, M.F. Synthesis of CO_2-responsive cellulose nanocrystals by surface-initiated Cu(0)-mediated polymerisation. *Green Chem.* **2017**, *19*, 4141–4152. https://doi.org/10.1039/c7gc01798g.
9. Anžlovar, A.; Huskić, M.; Žagar, E. Modification of nanocrystalline cellulose for application as a reinforcing nanofiller in PMMA composites. *Cellulose* **2016**, *23*, 505–518. https://doi.org/10.1007/s10570-015-0786-9.
10. Arredondo, J.; Woodcock, N.M.; Garcia-Valdez, O.; Jessop, P.G.; Champagne, P.; Cunningham, M.F. Surface modification of cellulose nanocrystals via RAFT polymerization of CO_2-responsive monomer-tuning hydrophobicity. *Langmuir* **2020**, *36*, 13989–13997. https://doi.org/10.1021/acs.langmuir.0c02509.
11. Eskandari, P.; Roghani-Mamaqani, H.; Salami-Kalajahi, M.; Abousalman-Rezvani, Z. Modification of cellulose nanocrystal with dual temperature- and CO_2-responsive block copolymers for ion adsorption applications. *J. Mol. Liq.* **2020**, *310*, 113234. https://doi.org/10.1016/j.molliq.2020.113234.
12. Du, X.; Zhang, Z.; Liu, W.; Deng, Y. Nanocellulose-based conductive materials and their emerging applications in energy devices—A review. *Nano Energy* **2017**, *35*, 299–320. https://doi.org/10.1016/j.nanoen.2017.04.001.
13. Xu, C.; Chen, W.; Gao, H.; Xie, X.; Chen, Y. Cellulose nanocrystal/silver (CNC/Ag) thin-film nanocomposite nanofiltration membranes with multifunctional properties. *Environ. Sci. Nano* **2020**, *7*, 803–816. https://doi.org/10.1039/c9en01367a.
14. Sucinda, E.F.; Abdul Majid, M.S.; Ridzuan, M.J.M.; Cheng, E.M.; Alshahrani, H.A.; Mamat, N. Development and characterisation of packaging film from Napier cellulose nanowhisker reinforced polylactic acid (PLA) bionanocomposites. *Int. J. Biol. Macromol.* **2021**, *187*, 43–53. https://doi.org/10.1016/j.ijbiomac.2021.07.069.
15. Qin, L.; Gao, H.; Xiong, S.; Jia, Y.; Ren, L. Preparation of collagen/cellulose nanocrystals composite films and their potential applications in corneal repair. *J. Mater. Sci. Mater. Med.* **2020**, *31*, 55. https://doi.org/10.1007/s10856-020-06386-6.
16. Cui, J.; Gao, P.; Deng, Y. Destruction of Per- A nd Polyfluoroalkyl Substances (PFAS) with Advanced Reduction Processes (ARPs): A Critical Review. *Environ. Sci. Technol.* **2020**, *54*, 3752–3766. https://doi.org/10.1021/acs.est.9b05565.
17. Domingo, J.L.; Nadal, M. Human exposure to per- and polyfluoroalkyl substances (PFAS) through drinking water: A review of the recent scientific literature. *Environ. Res.* **2019**, *177*, 108648. https://doi.org/10.1016/j.envres.2019.108648.
18. Gomri, C.; Tarek, B.; Chaix, A.; Dorandeu, C.; Chopineau, J.; Petit, E.; Aissou, K.; Cot, D.; Cretin, M.; Semsarilar, M. A facile approach to modify cellulose nanocrystal for the adsorption of perfluorooctanoic acid. *Carbohydr. Polym.* **2023**, *319*, 121189. https://doi.org/10.1016/j.carbpol.2023.121189.
19. Semsarilar, M.; Ladmiral, V.; Blanazs, A.; Armes, S.P. Cationic polyelectrolyte-stabilized nanoparticles via RAFT aqueous dispersion polymerization. *Langmuir* **2013**, *29*, 7416–7424. https://doi.org/10.1021/la304279y.
20. Zhu, W.; Yao, Y.; Zhang, Y.; Jiang, H.; Wang, Z.; Chen, W.; Xue, Y. Preparation of an Amine-Modified Cellulose Nanocrystal Aerogel by Chemical Vapor Deposition and Its Application in CO_2 Capture. *Ind. Eng. Chem. Res.* **2020**, *59*, 16660–16668. https://doi.org/10.1021/acs.iecr.0c02687.
21. Singh, S.; Dhakar, G.L.; Kapgate, B.P.; Maji, P.K.; Verma, C.; Chhajed, M.; Rajkumar, K.; Das, C. Synthesis and chemical modification of crystalline nanocellulose to reinforce natural rubber composites. *Polym. Adv. Technol.* **2020**, *31*, 3059–3069. https://doi.org/10.1002/pat.5030.
22. Anpilova, A.Y.; Mastalygina, E.E.; Khrameeva, N.P.; Popov, A.A. Methods for Cellulose Modification in the Development of Polymeric Composite Materials (Review). *Russ. J. Phys. Chem. B* **2020**, *14*, 176–182. https://doi.org/10.1134/S1990793120010029.
23. Zhang, D.; Luo, Q.; Gao, B.; Chiang, S.Y.D.; Woodward, D.; Huang, Q. Sorption of perfluorooctanoic acid, perfluorooctane sulfonate and perfluoroheptanoic acid on granular activated carbon. *Chemosphere* **2016**, *144*, 2336–2342. https://doi.org/10.1016/j.chemosphere.2015.10.124.